A Remedy to Losing Time Synchronization at D-PMUs, H-PMUs, and WMUs in Event Location Identification in Power Distribution Systems

Zong-Jhen Ye, *Student Member, IEEE*, Milad Izadi, *Member, IEEE*,
Mohammad Farajollahi, *Member, IEEE*, and Hamed Mohsenian-Rad, *Fellow, IEEE*

***Abstract*—Recent advancements in synchronized sensor technologies has introduced an unprecedented level of visibility in power distribution systems. Apart from the Distribution-level Phasor Measurement Units (D-PMUs), a.k.a. micro-PMUs, that have been widely used in recent years, other synchronized sensors have also been developed in this field, including Harmonic Phasor Measurement Units (H-PMUs) and Waveform Measurement Units (WMUs). However, in practice, it is common for these sensors to lose time synchronization over some periods of time and for different reasons. In this paper, we propose new and customized solutions to tackle loss of time synchronization in D-PMUs, H-PMUs, and WMUs, whereby addressing the unique challenges in each case. Our focus is on solving the event location identification problem, for different types of steady-state and transient events. We show that, our methods can maintain high accuracy in event location identification, despite losing time synchronization, whether we use D-PMUs, H-PMUs, or WMUs.**

***Keywords*: Synchronized measurements, losing time synchronization, power distribution system, event location identification, synchronization operator, D-PMUs, H-PMUs, WMUs, synchro-phasors, harmonic synchro-phasors, and synchro-waveforms.**

I. Introduction

A. Background and Motivation

Due to the major differences between power transmission systems and power distribution systems, such as limited instrumentation, unbalanced phases, and the complexity of the laterals [1], the accurate identification of the *location of an event* in power distribution systems is a very challenging task.

The recent advancements in developing sensor technologies with precise *time synchronization* has given a boost to this field to support new methods that take advantage of the time-synchronized measurements to significantly improve the accuracy of event location identification in power distribution systems. Importantly, different types of events must be studied by different types of time-synchronized measurements, which come from different types of advanced smart grid sensors:

- Distribution-level Phasor Measurement Units (D-PMUs): They provide *time-synchronized* measurements of the fundamental phasors of voltage and current [2], [3]. Measurements from D-PMUs have been used to identify the location of the events that create a *sustained* change in the *fundamental* components of voltage or current, such as a Capacitor Bank Switching, e.g., see [4], [5].
- Harmonic Phasor Measurement Units (H-PMUs): They provide *time-synchronized* measurements of not only the fundamental phasors but also the *harmonic* phasors [6]–[9]. Measurements from H-PMUs have been used to identify the location of the events that create a *sustained* change in the *harmonic* components of voltage or current, such as a High Impedance Fault (HIF) [10], [11].
- Waveform Measurement Units (WMUs): They provide *time-synchronized* measurements of the *raw samples* of voltage and current. Unlike the measurements from D-PMUs and H-PMUs that are in phasor domain, the measurements from WMUs are in time domain [12]–[18]. WMUs have been used to identify the location of those events that create a *transient* change in voltage and/or in current over a very short period of time, often less than a cycle, such as a sub-cycle Incipient Fault. [15].

Importantly, the key to the success of the above (and similar) event location identification methods is that they use *time-synchronized* measurements from multiple locations during the occurrence of the event. Time synchronization in advanced smart grid sensors is typically achieved by using the Global Positioning System (GPS). However, it is common for smart grid sensor devices to experience losing the GPS signals. For example, the study in [19], [20] has shown that over 70% of the PMUs in practice suffer from GPS Signal Loss (GSL) on a daily basis. It is worth mentioning that, the details on how a sensor may detect GSL is explained in details in [20], which is according to the existing IEEE Standards. When GSL happens, it can affect the accuracy of the event location methods that directly rely on the time synchronization among the measurements that they receive from different sensors.

Thus, in this paper, we raise the following questions: **1)** If we lose time synchronization among the sensors, then how does it affect the accuracy of the event location identification task? **2)** How can we address such scenario and improve the existing methods such that we can accurately obtain the location of different types of events *despite losing time synchronization* in the above three classes of advanced sensors?

B. Summary of Contributions

We seek to answer the above questions in this paper. The contributions of this paper are summarized as follows:

1) The impact of losing time synchrnozation in sensor measurements is systematically investigated in the context of event location identification problem in power distribution systems. Depending on the type of an event, and the type of the measurements that are needed to identify the location of the event, our analysis encompasses different

The authors are with the Department of Electrical and Computer Engineering, University of California, Riverside, CA, USA. The corresponding author is H. Mohsenian-Rad, e-mail: hamed@ece.ucr.edu.

types of advanced smart grid sensors. The scope of this analysis is comprehensive and considers a wide range of events, including switching actions, high-impedance faults, incipient faults, and transient sub-cycle events.

2) The proposed methods provide customized solutions to tackle losing time synchronization among D-PMUs, H-PMUs, and WMUs. The overarching idea is to define and estimate proper synchronization operators among each type of sensors, to achieve *comparable* forward sweep and backward sweep calculations based on the measurements from different sensors. The analysis is done by using closed-form solutions and by conducting regression analysis, in *phasor-domain* and in *time-domain*, based on the fundamental phasor measurements, harmonic phasor measurements, and raw waveform measurements. The challenges are addressed in each case. The relationships across these cases are also discussed.
3) Through various case studies, it is shown that, losing time synchronization among the sensors can *significantly degrade* the performance of the existing methods in correctly identifying the location of various events. However, it is shown that, our proposed methods are highly capable to remedy this issue in various cases, whether we use D-PMUs, H-PMUs, and WMUs.

C. Literature Review

There is a rich literature on location identification of events, such as for ground faults [21], capacitor bank switching [4], high impedance faults [10], [11], and transient events [15], [22]. Many of these methods use measurements from *multiple* sensors, i.e., synchro-phasors and synchro-waveforms. They inherently assume that the measurements are time-synchronized. However, when GSL occurs, the sensors (i.e., D-PMUs, H-PMUs, or WMUs) must rely on their own internal crystal oscillators to estimate time. These internal clocks are prone to various errors, caused by the changes in the operation temperature, voltage, aging, etc [23], [24]. For example, it is reported in [19] that, during a GSL period, they observed over 26 microseconds drift in time synchronization, which is equivalent to 0.57 degrees at the fundamental frequency.

To mitigate the impact of losing time synchronization, in [25], the phase angle data was used from synchronized phasor measurements to compensate for the phase angles at unsynchronized measurements. In [26], a high sampling rate of up to 100 kHz was used to combine the traveling wave method with Hilbert-Huang transform and a convolutional neural network, to deal with the issue of losing time synchronization. In [27], the authors used unsynchronized low voltage measurements to estimate the faulted segments in the medium voltage systems.

There are also some very recent methods that have looked into using the concept of *synchronization operator* to deal with losing time synchronization. In the conference version of this submission in [28], we proposed a method to improve the accuracy of event location identification when we lose time synchronization among D-PMUs. In this journal version, we not only enhance the method in [28], but also significantly expand it to address the similar challenges in H-PMUs and WMUs, which requires tackling several new challenges. Similar operators are also considered in [29]–[31] but exclusively for fault locations using PMU measurements, where the focus in [29], [30] is on transmission systems. In this paper, we consider different types of events, beyond ordinary faults. We also cover not only D-PMUs but also H-PMUs and WMUs.

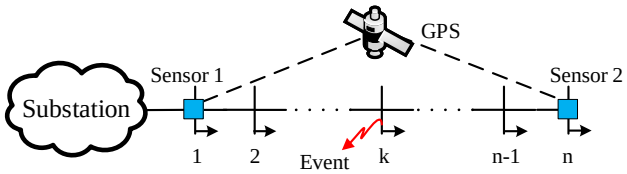

Fig. 1. A power distribution system with n buses and two time-synchronized sensors. An event occurs at *unknown* bus k. The two sensors can be a pair of D-PMUs (Section II), H-PMUs (Section III), or WMUs (Section IV).

II. Losing Time Synchronization in D-PMUs

Consider the power distribution system in Fig. 1. For the ease of discussion, we assume that the feeder does not have any lateral. The case where the feeder has laterals will be discussed in Section V. There are n buses in the network in Fig. 1. Two sensors are installed on this feeder, one at the beginning of the feeder at bus 1, and one at the end of the feeder at bus n. The sensors can be a pair of D-PMUs (as we assume in this section), a pair of H-PMUs (in Section III), or a pair of WMUs (in Section IV). For the rest of this section, we assume that the event at bus k has a *steady-state* impact on the *fundamental* components of the voltage and/or current.

If the two D-PMUs are *time-synchronized*, then their measurements can be used to accurately identify the location of the event, e.g., see [4], [29], [32]. In this section, we will first briefly overview how the phasor measurements from D-PMU 1 and D-PMU 2 can be used to identify the location of the event if the two D-PMUs *maintain time synchronization*. After that, we will develop a method to provide a remedy to *losing time synchronization* between the two D-PMUs.

A. Time Synchronization is Maintained

Suppose V_1^{before} and I_1^{before} denote the voltage and current phasors that are measured by D-PMU 1 during the steady-state conditions *before* the event happens. Suppose V_1^{after} and I_1^{after} denote the voltage and current phasors that are measured by D-PMU 1 during the steady-state conditions *after* the event happens. We define the *differential* phasors at D-PMU 1 as:

$$\begin{aligned} V_1 &= V_1^{\text{after}} \quad V_1^{\text{before}}; \\ I_1 &= I_1^{\text{after}} \quad I_1^{\text{before}}. \end{aligned} \tag{1}$$

We can similarly obtain V_n and I_n based on the measurements by D-PMU 2 at bus n. As explained in details in [4], we can use V_1 and I_1 from D-PMU 1 to apply the Kirchhoff's Current Law (KCL) and the Ohm's Law to conduct a *forward* sweep, which starts from bus 1 and ends at bus n, to obtain the differential voltage phasors at each bus:

$$V_p^f = V_{p-1}^f + Z_{p-1} \quad I_{p-1}^f; \quad p = 2; \quad ; n; \tag{2a}$$

$$I_p^f = I_{p-1}^f + Y_p \quad V_p^f; \quad p = 2; \quad ; n \quad 1; \tag{2b}$$

where p denotes the bus number of the forward nodal voltage in (2a) and the starting bus for the line current in (2b). Similarly, we can use V_n and I_n from D-PMU 2 to conduct a *backward* sweep which starts from bus n and ends at bus 1, to obtain the differential voltage phasors at each bus:

$$V^b_{p-1} = V^b_p + Z_{p-1} I^b_{p-1}; \quad p = 2; \quad ; n; \tag{3a}$$

$$I^b_{p-1} = I^b_p + Y_p V^b_p; \quad p = 2; \quad ; n \quad 1: \tag{3b}$$

Superscript f in (2) denotes the forward sweep, and the superscript b in (3) denotes the backward sweep. Notations $Z_1; Z_2; : : : ; Z_{n-1}$ denote the line impedances, and notations $Y_1; Y_2; : : : ; Y_{n-1}$ denote the admittances of the loads at each bus. These parameters are assumed to be known.

Under *synchronized* measurements, the voltage from the forward nodal calculations in (2a) and those from the backward nodal calculations in (3a) are not similar, except at the event bus k. Therefore, one can derive the unknown event bus k by solving the following optimization problem [4]:

$$k^? = \arg\min_p \quad V^f_p \quad V^b_p : \tag{4}$$

Note that, if the measurements are perfect, the network model is perfect, and the time synchronization is also perfect, then the phasor difference in the objective function in (4) would be zero at the event bus. However, in practice, such difference is not zero, due to imperfection in the above various factors. Importantly, the exact value of such difference is *not* a concern here; because we simply look for the minimum of the difference across the buses, weather such minimum is zero or non-zero. Another note to mention is that, the exact amount of such minimum is *not* the focus in the above optimization problem. That is why we use $argmin$, instead of min, in the above formulation. For more details, please refer to [4].

B. Remedy to Losing Time Synchronization

Next, suppose D-PMU 1 and D-PMU 2 lose time synchronization. Recall from Section I-C that, this can result in considerable error in the *relative* phase angle between D-PMU 1 and D-PMU 2. Thus, the forward nodal voltage calculations in (2a) and the backward nodal voltage calculations in (3a) may *not* lead to similar results *even in the absence* of an event. Therefore, we can no longer use the formulation in (4) to accurately estimate the location of the event.

For the rest of this section, we seek to modify the formulation in (4) to achieve an accurate estimation of the location of the event, *despite* the drift in the time synchronization between D-PMU 1 and D-PMU 2. First, we hypothetically tune the two D-PMUs into synchronized measurements by using a *synchronization operator*, which is defined in [32] as:

$$V^f_p = e^{j \ 1} \quad V^b_p; \tag{5}$$

where $_1$ is the *offset* in the relative *phase angle* in the *fundamental* component at D-PMU 2 compared to the *fundamental* component at D-PMU 1. This offset is caused due to losing time synchronization between the two sensors.

Importantly, $_1$ is *not* known in practice. Thus, we must find a way to solve the following revised optimization problem:

$$k^? = \arg\min_{p; \ 1} \quad V^f_p \quad V^b_p e^{j \ 1} : \tag{6}$$

There are *two unknowns* in the above optimization problem. One unknown is the event bus. The other unknown is the offset in the phase angle due to losing time synchronization.

In order to solve the minimization problem in (6), we need another set of physical equations that could help us *eliminate* parameter $_1$ as an optimization variable in (6). This would help us express (6) in a form that is similar to (4), such that we can directly obtain the unknown event bus $k^?$. Next, we propose two approaches to address this issue.

Approach 1: At any bus k, and based on the measurements right *before* the event occurs, we can write:

$$V^{f; \text{ before}}_p = e^{j \ 1} V^{b;\text{before}}_p \quad) \quad e^{j \ 1} = \frac{V^{f; \text{ before}}_p}{V^{b;\text{before}}_p} \quad ; \tag{7}$$

where

$$\begin{aligned} V^{f; \text{ before}}_p &= V^{f; \text{ before}}_{p-1} + Z_{p-1} I^{f; \text{ before}}_{p-1}; \quad p = 2; \quad ; n; \\ V^{b;\text{before}}_{p-1} &= V^{b;\text{before}}_p + Z_{p-1} I^{b;\text{before}}_{p-1}; \quad p = 2; \quad ; n: \end{aligned} \tag{8}$$

Here, $V^{f; \text{ before}}_p$ is the result of the forward nodal voltage calculations based on measuring V^{before}_1 and I^{before}_1 at D-PMU 1; and $V^{b;\text{before}}_p$ is the result of the backward nodal voltage calculations based on measuring V^{before}_n and I^{before}_n at D-PMU 2. While the expressions in (2), (3), and (4) are in *differential* mode, as defined in (1), the expressions in (7) and (8) are in *regular* mode, based on the phasors *before* the event occurs.

By substituting (7) into (6), we can now express (6) as an optimization problem over p as the *only* variable:

$$k^? = \arg\min_p \quad V^f_p \quad V^b_p \quad \frac{V^{f; \text{ before}}_p}{V^{b;\text{before}}_p} \quad : \tag{9}$$

Thus, we can identify the location of the event *despite* the fact that D-PMU 1 and D-PMU 2 have lost time synchronization.

Approach 2: Theoretically, the expression in (7) should be the same for each bus p before an event occurs. However, (7) can slightly drift; because (8) could underestimate or overestimate the voltage at the end or the beginning of a branch as we do the forward sweep or backward sweep, respectively. To deal with this issue, we use a *regression* method to estimate the synchronization operator. Here, instead of estimating $e^{j \ 1}$ based on (7) at each bus, we solve the following Least Square (LS) problem across all the n buses in the network:

$$\min_{1} \quad \begin{bmatrix} V^{f; \text{ before}}_1 \\ \vdots \\ V^{f; \text{ before}}_n \end{bmatrix} \quad \begin{bmatrix} V^{b;\text{before}}_1 \\ \vdots \\ V^{b;\text{before}}_n \end{bmatrix} e^{j \ 1} \quad ; \tag{10}$$

Note that, similar to the formulation in (7), the formulation in (10) obtains $_1$ based on the regular, i.e., not differential, phasor measurements. Importantly, we can obtain a *closed-form* solution for the optimization problem in (10) as:

$$e^{j\,\theta_1} = \begin{bmatrix} V_1^{b;\text{before}} \\ \vdots \\ V_n^{b;\text{before}} \end{bmatrix}^{T} \begin{bmatrix} V_1^{b;\text{before}} \\ \vdots \\ V_n^{b;\text{before}} \end{bmatrix}^{-1} \begin{bmatrix} V_1^{b;\text{before}} \\ \vdots \\ V_n^{b;\text{before}} \end{bmatrix}^{T} \begin{bmatrix} V_1^{f;\,\text{before}} \\ \vdots \\ V_n^{f;\,\text{before}} \end{bmatrix}. \tag{11}$$

By substituting (11) into (6), we can now express (6) as an optimization problem over p as the only variable:

$$k^{?} = \arg\min_{p} \left| V_p^f - V_p^b \begin{bmatrix} V_1^{b;\text{before}} \\ \vdots \\ V_n^{b;\text{before}} \end{bmatrix}^{T} \begin{bmatrix} V_1^{b;\text{before}} \\ \vdots \\ V_n^{b;\text{before}} \end{bmatrix}^{-1} \begin{bmatrix} V_1^{b;\text{before}} \\ \vdots \\ V_n^{b;\text{before}} \end{bmatrix}^{T} \begin{bmatrix} V_1^{f;\,\text{before}} \\ \vdots \\ V_n^{f;\,\text{before}} \end{bmatrix} \right|. \tag{12}$$

Before we end this section, we point out that, the formulations in (6), (9), and (12) are based on an implicit assumption that, while θ_1 is unknown, it does *not* change *during* the event. This is a valid assumption; because most events take only a short period of time, often only fraction of a second [3], [14].

III. Losing Time Synchronization in H-PMUs

Suppose the two sensors in Fig. 1 are H-PMUs. H-PMUs provide time-synchronized measurements of not only the fundamental phasors but also the harmonic phasors. Accordingly, H-PMUs are particularly helpful to identify the location of the events that create a *sustained* change in the *harmonic* component of the voltage and/or current, such as HIFs.

Importantly, there are some subtle points about how losing time synchronization can affect the harmonic phasor measurements. This can be understood by examining the graphs in Fig. 2. First, consider the distorted waveforms in Fig. 2(a). Suppose the blue curve is the true distorted waveform and the red curve is the *time drifted* distorted waveform. Here, the time drift is the result of *losing time synchronization* in the sensor. The decomposition of the original distorted waveform into its fundamental component, its third harmonic component, and its fifth harmonic component are shown in Figs. 2(b), (c), (d), respectively. Specifically, let us define θ_1, θ_3 and θ_5 as the angle difference at the fundamental frequency, the third harmonic order and the fifth harmonic order, respectively. From the graphs in Fig. 2, it is clear that:

$$\theta_1 \neq \theta_3 \neq \theta_5. \tag{13}$$

This is because, although the time drift is the same for the fundamental and harmonic waveforms in *time domain*, it has different representations in the phasors in *frequency domain*.

The above note, along with some other technical complications, create major differences between handling lack of time-synchronization among D-PMUs, which we covered in Section II, in comparison with handling lack of time synchronization among H-PMUs, which we will cover in this section.

A. Time Synchronization is Maintained

Let us introduce a new subscript h to mark the harmonic order of the the harmonic component. Based on the analysis in [4], [33], we can use the measurements from the two H-PMUs to identify the location of the event by solving the following optimization problem that is defined at harmonic order h:

$$k^{?} = \arg\min_{p} \quad V_{p;h}^f - V_{p;h}^b \; . \tag{14}$$

If we use phasor measurements of different harmonic components, then we can sum up the terms over the harmonic orders to identify the location of the events as follows:

$$k^{?} = \arg\min_{p} \sum_{h=1;3;5} V_{p;h}^f - V_{p;h}^b \; ; \tag{15}$$

where $V_{p;h}^f$ and $I_{p;h}^f$ are obtained through backward and forward sweep calculations for each harmonic component, somewhat similar to (8). However, one key note to consider here is that, all the impedances and all the admittances in the forward and backward sweep calculations for H-PMU measurements must take into account the impact of the harmonics. For example, if we use $Z_p = R_p + j\,!\,L_p$ in (8), then we should use $Z_{p;h} = R_p + j\,h\,!\,L_p$ in the forward and backward sweep calculations for H-PMU measurements.

B. Remedy to Losing Time Synchronization

If H-PMU 1 and H-PMU 2 lose time synchronization, then we can no longer use (14) or (15) to obtain the location of the event based on the harmonic phasor measurements. However, similar to Section II.B, we can hypothetically tune the measurements from H-PMU 1 and H-PMU 2 into synchronized measurements by using proper *synchronization operators*.

Let θ_h denote the drift in the relative phase angle between H-PMU 1 and H-PMU 2 at harmonic order h. Accordingly, we denote $e^{j\,\theta_h}$ as the synchronization operator for harmonic order h. As it is evident from Fig. 2, we must use a different synchronization operator for each harmonic order. To the best of our knowledge, the concept of synchronization operators have *not* been previously discussed in the literature in the context of harmonic phasor measurements.

Next, we discuss two different approaches to obtain the synchronization operators for harmonic phasors measurements when H-PMU 1 and H-PMU 2 lose time synchronization. As we will see in the case studies, each of these methods may have some advantages under certain circumstances in the analysis.

Approach 1: This approach is applicable *only if* the voltage at H-PMU 1 and the voltage at H-PMU 2 include considerable presence of harmonics *before* the event occurrence. Only in that case, we can repeat the same methodology that we proposed in Section II-B, but this time to estimate θ_h for a given harmonic order h. In this scenario, we can remedy the impact of losing time synchronization in the optimization problem in (14) by using the following formulation:

$$k^{?} = \arg\min_{p} \sum_{h=1;3;5} V_{p;h}^f - V_{p;h}^b \; \frac{V_{p;h}^{f;\,\text{before}}}{V_{p;h}^{b;\text{before}}} \; ! \; : \tag{16}$$

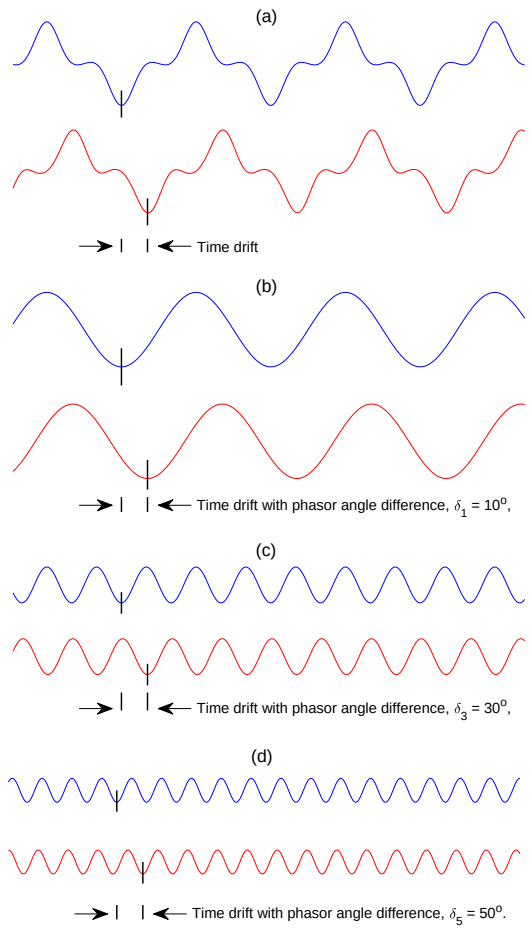

Fig. 2. The impact of losing time synchronization between H-PMU 1 (blue) and H-PMU 2 (red) on the amount of the drift in their relative phase angle at different harmonic orders: (a) the original distorted waveform; (b) the fundamental component; (c) the third harmonic; and (d) the fifth harmonic. While the time drift is the same across all four graphs, the drifts in the relative phase angle is not the same across different harmonic orders.

where $V^{f}_{p;h}$ is the result of the forward nodal voltage calculations based on measuring $V^{\text{before}}_{1;h}$, and $I^{\text{before}}_{1;h}$ at H-PMU 1; and $V^{b}_{p;h}$ is the result of the backward nodal voltage calculations based on measuring $V^{\text{before}}_{n;h}$ and $I^{\text{before}}_{n;h}$ at H-PMU 2:

$$\begin{aligned} V^{f;\,\text{before}}_{p;h} &= V^{f;\,\text{before}}_{p-1;h} + Z_{p-1;h}\, I^{f;\,\text{before}}_{p-1;h}; \quad p = 2; \quad ; n; \\ V^{b;\text{before}}_{p-1;h} &= V^{b;\text{before}}_{p;h} + Z_{p-1;h}\, I^{b;\text{before}}_{p-1;h}: \quad p = 2; \quad ; n: \end{aligned} \tag{17}$$

Formulation (16) is the extension of (9). We can similarly extend (12) to express it based on the harmonic phasor measurements from H-PMU 1 and H-PMU 2. We shall clarify that, the formulation in (16) would include *only* those harmonics that exist both before and after the event occurs. For example, if the third and the fifth harmonics are present *before* the event occurs, and the third and the seventh harmonics are present *after* the event occurs, then we formulate (16) *only* based on the third harmonic that is present both before and after the event occurs, and not based on the fifth or seventh harmonics.

Approach 2: Unlike Approach 1 that requires the presence of the harmonics *both* before the event occurrence, Approach 2 is always applicable. However, before we explain Approach 2, let us further elaborate the limitations of Approach 1. To see such limitations, consider a power distribution system that has no harmonic distortion. Suppose an event occurs that creates third harmonics in the system. Since the event causes steady state third harmonics, it is well-suited to be examined by H-PMUs. Thus, one may seek to use (16) to identify the location of the harmonic source. However, since the harmonic source did *not* exist prior to the event, we have:

$$V^{\text{before}}_{1;h} = V^{\text{before}}_{n;h} = 0; \quad I^{\text{before}}_{1;h} = I^{\text{before}}_{n;h} = 0: \tag{18}$$

Therefore, we have:

$$V^{b;\text{before}}_{p;h} = V^{f;\,\text{before}}_{p;h} = 0; \quad p = 1; : : ; n: \tag{19}$$

Thus, we *cannot* estimate $_h$ by using (16); because it would cause a division by zero. Hence, Approach 1 is not applicable.

Importantly, we *cannot* resolve the above issue by using the harmonic phasor measurements *after* the event occurs instead of using the harmonic phasor measurements *before* the event occurs. It does *not* help. To see why, note that, if the harmonic phasors do not exist before the event occurs, then we have:

$$V^{f}_{p;h} = V^{f;\,\text{after}}_{p;h}; \qquad V^{b}_{p;h} = V^{b;\text{after}}_{p;h} \tag{20}$$

where $V^{f;\,\text{after}}_{p;h}$ is the result of the forward nodal calculations based on the harmonic phasor measurements *after* the event happens, and $V^{b;\text{after}}_{p;h}$ is the result of the backward nodal calculations based on the harmonic phasor measurements *after* the event occurs. Therefore, even if we define (16) based on the harmonic phasor measurements *after* the event occurs, we end up expressing the formulation inside $j\ j$ in (16) as follows:

$$\begin{aligned} V^{f}_{p;h} \qquad V^{b}_{p;h} \quad \frac{V^{f;\,\text{after}}_{p;h}}{V^{b;\text{after}}_{p;h}}\,! \quad &= V^{f;\,\text{after}}_{p;h} \quad \cancel{V^{b;\text{after}}_{p;h}} \quad \frac{V^{f;\,\text{after}}_{p;h}}{\cancel{V^{b;\text{after}}_{p;h}}}\,! \\ &= V^{f;\,\text{after}}_{p;h} \quad V^{f;\,\text{after}}_{p;h} \\ &= 0: \end{aligned} \tag{21}$$

Therefore, we need a method to obtain $_h$ without using the harmonic phasor measurements. In this regard, we propose to use the following fundamental relationship:

$$_h = h \quad _1: \tag{22}$$

For example, we have $_3 = 3 \quad _1$ and $_5 = 5 \quad _1$. Note that, $_h$ and $_1$ must be in radian for the relation in (22) to hold.

In order to show how to derive the relationship in (22), consider the following general formulation for a distorted voltage waveform during steady-state conditions [14, ch. 4.1.1]:

$$v_h(t) = \sum_{h=1}^{\infty} p\ \overline{2} V_h \cos(h\,!\,t + \quad _h); \tag{23}$$

where V_h and $_h$ are the magnitude and phase angle of harmonic order h, respectively; and $!$ is the fundamental

angular. If the waveform in (23) is delayed by Δ in time domain, then we can express it as follows:

$$\begin{aligned} v_h(t+\Delta) &= \sum_{h=1}^{\infty} \sqrt{2} V_h \cos(h\omega_1(t+\Delta)+\theta_h) \\ &= \sum_{h=1}^{\infty} \sqrt{2} V_h \cos(h\omega_1 t + h\omega_1\Delta + \theta_h) \\ &= \sum_{h=1}^{\infty} \sqrt{2} V_h \cos(h\omega_1 t + h\theta_1 + \theta_h) \\ &= \sum_{h=1}^{\infty} \sqrt{2} V_h \cos(h\omega_1 t + \theta_h + \theta_h). \end{aligned} \tag{24}$$

By comparing the last two equalities, we can conclude (22).

From (7) and (22), we can obtain the following expression for the drift term at harmonic order h:

$$e^{j\theta_h} = e^{jh\theta_1} = \left(\frac{V_p^{f;\,\text{before}}}{V_p^{b;\text{before}}}\right)^h. \tag{25}$$

We can now express the following optimization problem over p as the *only* variable to obtain the location of the event:

$$k? = \arg\min_p \sum_{h=1,3,5} \left| V_{p;h}^f \quad V_{p;h}^b \left(\frac{V_p^{f;\,\text{before}}}{V_p^{b;\text{before}}}\right)^h \right|. \tag{26}$$

It is evident that, unlike the formulation in (16), the formulation in (26) does *not* require the harmonic distortions of harmonic order h to be present before the event occurs.

To better see the difference between (16) and (26), let us consider an example. Suppose there is no harmonic in the measurements before an event occurs. Suppose an event causes the third harmonic to appear. In this example, there is no harmonic *before* the event, but there is the third harmonic *after* the event. However, since the third harmonic is *not* present *both* before and after this event, we *cannot* use (16); because we *cannot* obtain $V_{p;h}^{f;\,\text{before}} = V_{p;h}^{b;\text{before}}$. Yet we *can* use (26); because we *can* obtain $V_p^{f;\,\text{before}} = V_p^{b;\text{before}}$, which only depends on the fundamental phasors. Accordingly, we can obtain $(V_p^{f;\,\text{before}} = V_p^{b;\text{before}})^3 = (V_p^{f;\,\text{before}} \quad V_p^{f;\,\text{before}} \quad V_p^{f;\,\text{before}}) = (V_p^{b;\text{before}} \quad V_p^{b;\text{before}} \quad V_p^{b;\text{before}})$ and solve (26).

IV. Losing Time Synchronization in WMUs

D-PMUs (Section II) and H-PMUs (Section III) are both designed to report *phasor* measurements. Therefore, they are both inherently incapable of properly capturing the events that cause distortions in voltage and/or current waveforms over only a *very short* period of time, such as during only a *fraction of a cycle*. Importantly, such *sub-cycle* events are sometimes critical to be investigated, such as when they indicate *incipient faults* in various power system apparatus and equipment.

Such sub-cycle events can be captured by WMUs, which provide time-synchronized voltage and current waveform measurements, also known as *synchro-waveforms* [14, Section 4.6], [12], [13], [15], [17]. WMUs operate at a very high reporting rate, such as 256 samples per cycle. This is much higher than the reporting rate of D-PMUs and H-PMUs that report at most two samples per cycle. Therefore, in this section, we focus on the application of WMUs in event location identification. Hence, we assume that the two sensors in Fig. 1 are WMUs. Accordingly, we focus on the analysis of *transient* and *sub-cycle* events. An example for such event is shown in Fig. 3. Notice the *momentary* damping oscillations in the voltage waveform that quickly disappear.

A. Time Synchronization is Maintained

Let $v_1(t)$ denote the voltage waveform and $i_1(t)$ denote the current waveform that are measured by WMU 1. Also, let $v_2(t)$ denote the voltage waveform and $i_2(t)$ denote the current waveform that are measured by WMU 2. Suppose a transient event occurs at unknown bus k. As shown in [15], if the waveform measurements from two WMUs remain time-synchronized, then we can use $v_1(t)$, $v_2(t)$, $i_1(t)$, and $i_2(t)$ to accurately identify the location of the event. In this method, first, the oscillatory modes of the transient components of synchronized waveform are characterized by conducting a modal analysis, where we express each waveform, starting from the moment when the event happens, as a summation of *damping sinosoidal terms*, e.g., by using the Prony transformation [7, Section 4.6.2]. Of particular interest is to approximately express each voltage and current waveform as a summation of a *fundamental* waveform and a dominant *event* waveform. For example, we can express $v_1(t)$ as:

$$\begin{aligned} v_1(t) \quad & V_1 \cos(\omega_1 t + \theta_1) + \\ & V_{1;\text{event}} e^{-\sigma_{\text{event}}(t)} \cos(\omega_{\text{event}} t + \theta_{1;\text{event}}). \end{aligned} \tag{27}$$

Here, the dominant mode of the transient event is represented by magnitude $V_{1;\text{event}}$, phase angle $\theta_{1;\text{event}}$, damping factor σ_{event}, and angular frequency ω_{event}. Importantly, we must use *multi-signal* modal analysis to obtain the *same* frequency ω_{event} and the *same* damping coefficient σ_{event} for the dominant event mode across the four synchronized waveforms in (29); see [15, Section II-A] for details about multi-signal modal analysis.

Next, the power distribution circuit is analyzed at the above extracted dominant event mode, to conduct the forward sweep and the backward sweep in order to obtain:

$$\begin{aligned} V_{p;\text{event}}^f &= V_{p-1;\text{event}}^f + Z_{p-1;\text{event}}\, I_{p-1;\text{event}}^f, \quad p = 2; \quad ; n; \\ I_{p;\text{event}}^f &= I_{p-1;\text{event}}^f + Y_{p;\text{event}}\, V_{p;\text{event}}^f, \quad p = 2; \quad ; n \quad 1; \\ V_{p-1;\text{event}}^b &= V_{p;\text{event}}^b + Z_{p-1;\text{event}}\, I_{p-1;\text{event}}^b, \quad p = 2; \quad ; n; \\ I_{p-1;\text{event}}^b &= I_{p;\text{event}}^b + Y_{p;\text{event}}\, V_{p;\text{event}}^b, \quad p = 2; \quad ; n \quad 1; \end{aligned} \tag{28}$$

where $V_{p;\text{event}}^f$ and $I_{p;\text{event}}^f$ denote the voltage and current phasor representations at the *event mode* in the forward sweep; and $V_{p;\text{event}}^b$ and $I_{p;\text{event}}^b$ denote the voltage and current phasor representations at the *event mode* in the backward sweep. In *event mode*, the line impedance is $Z_{p;\text{event}} = R_p \quad _{\text{event}} L_p + j\omega_{\text{event}} L_p$ and the admittance of load is $Y_{p;\text{event}} = 1/(R_p \quad _{\text{event}} L_p + j\omega_{\text{event}} L_p)$. Accordingly, the location of the transient event is identified as [15].

$$k? = \arg\min_p \left| V_{p;\text{event}}^f \quad V_{p;\text{event}}^b \right|. \tag{29}$$

Unlike in (4) in Section II, the backward and forward calculations in (29) are obtained from the dominant event mode that is extracted from the waveform measurements in time domain.

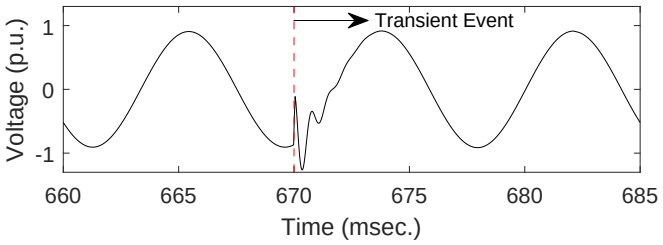

Fig. 3. Example of a short transient event as seen by a WMU.

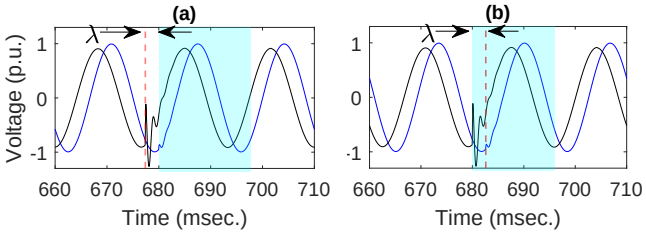

Fig. 4. There are two possible ways to select the time window to conduct the multi-signal modal analysis when the two WMUs lose time synchronization: (a) the window starts from the start of the event at WMU 1, the dashed line shows the start of the event at WMU 2, and we have $= -2.604$ msec; (b) the window starts from the start of the event at WMU 2, the dashed line shows the start of the event at WMU 1, and we have $= +2.604$ msec.

B. Remedy to Losing Time Synchronization

If WMU 1 and WMU 2 lose time synchronization, then we can no longer use (29) to identify the location of the event. This is due to the fact that, under the loss of time synchronization, the event mode of the waveform measurements is obtained *incorrectly*, because it is obtained based on *incorrect time window in the modal analysis*. For example, consider the voltage waveform measurements in Fig. 4. The *true start time* of the event is at $t = 680$ msec. Suppose WMU 1 is used as the reference to select the time window for the purpose of multi-signal modal analysis. Accordingly, the light blue rectangle in Fig. 4(a) is considered. Thus, as far as the calculation of the event mode is concerned, the voltage waveform from WMU 2 is drifted by $= 2.604$ msec relative to the voltage waveform at WMU 1. Next, suppose WMU 2 is used as the reference to select the time window for the purpose of the multi-signal modal analysis. Accordingly, the light blue rectangle is in Fig. 4 (b). Thus, as far as the calculation of the event mode is concerned, the voltage waveform from WMU 2 is drifted by $= +2.604$ msec relative to the voltage waveform at WMU 1. In either case, a significant part of the voltage waveform inside the window is *not* related to the event signature. Accordingly, the result of the modal analysis of the voltage waveform will *not* be correct anymore.

Importantly, we *cannot* fix the above issue by adding a shift to phase angle at one sensor in frequency domain, as we did in Section II for D-PMUs and in Section III for H-PMUs. Instead, we need to fix the issue in time domain before we apply the modal analysis. This can be done in three steps.

Step 1: We estimate $_1$ as the drift in the relative phase angle in the fundamental phasor, using (11) in Section II. Given $_1$, we then obtain the following delay factor in time domain:

$$= \frac{T}{2} \quad _1; \tag{30}$$

where T is the length of one cycle of the fundamental component. Since WMUs provide the raw voltage waveforms, we can obtain the fundamental component by applying the Fourier Transform. Thus, obtaining $_1$ by using the methods in Section II is readily available. That is why the period of the fundamental component is used in (30). As an example, for the voltage waveforms in Fig. 4 (a), if we apply (11) to the waveforms, then $_1$ is estimated as 0.981 radian. Since $T = 16.67$ msec for the fundamental component, we obtain

$$= 16.67 \quad (\quad 0.981)=2 \quad = \quad 2.602\text{msec}; \tag{31}$$

which is almost the same as the true time delay 2.604 msec between the waveforms from the two WMUs that we mentioned earlier in this section. As we will see in Section VI in our case studies, the above estimation is very robust.

Step 2: Once is estimated, the next step is to *align* the waveform measurements at WMU 2 with the waveform measurements at WMU 2 by shifting them according to :

$$v_2^{\text{aligned}}(t) = v_2(t + \quad); \quad i_2^{\text{aligned}}(t) = i_2(t + \quad): \tag{32}$$

For example, since based on (31), we estimate $= 2.602$ msec in Fig. 4(a), we set $v_2^{\text{aligned}}(t) = v_2(t \quad 2.602)$ and $i_2^{\text{aligned}}(t) = i_2(t \quad 2.602)$. These new waveforms are approximately synchronized with the waveforms at WMU 1, i.e., with $v_1(t)$ and $i_1(t)$, for the purpose of event location identification.

Step 3: Instead of using $v_1(t)$, $v_2(t)$, $i_1(t)$, and $i_2(t)$, we use the following waveforms to in a multi-signal modal analysis:

$$v_1(t); v_2^{\text{aligned}}(t); i_1(t); i_2^{\text{aligned}}(t): \tag{33}$$

Accordingly, the minimization in (29) is changed to:

$$k^? = \arg\min_p \quad V^f_{\text{p, event}} \quad V^{\text{aligned};b}_{\text{p, event}} \; : \tag{34}$$

V. Extensions and Further Discussions

In this section, we discuss two extensions of the proposed method, namely the case where there are more than two sensors available, and the case where the network is unbalanced.

A. Using Multiple Sensors

We can extend our approach to address the case where the network includes laterals and multiple sensors. Specifically, we assume that the power distribution system has $m \quad 1$ laterals and $m+1$ sensors. The sensors are installed at the substation, at the end of the main, and at the end of the $m \quad 1$ laterals. An example is shown in Fig. 5, based on the IEEE 33 bus test system, where $m = 4$. The network has $m \quad 1 = 3$ laterals and $m + 1 = 5$ sensors. Throughout this section, we assume that the sensors are D-PMUs. The ideas for the extensions to multiple sensors where the sensors are H-PMUs and WMUs are similar and not explained due to space limitation.

First, suppose the D-PMUs maintain time synchronization. We can extend the method in (4) to include all the D-PMUs:

$$k^? = \arg\min_p \sum_{i=2}^{m+1} \quad V_p^{f\,(1;i)} \quad V_p^{b(1;i)} \; ; \tag{35}$$

where the superscript $f(1;i)$ is associated with the forward sweep between D-PMU 1 and D-PMU i, and $b(1;i)$ is associated with the backward sweep between D-PMU 1 and D-PMU i. Note that, as a special case, when $m = 1$ and $i = 2$, the minimization in (35) reduces to the minimization in (4).

Next, suppose we lose time synchronization among the D-PMUs. We can use an analysis similar to the one in (12) to estimate the synchronization operator between any two D-PMUs. In particular, we can estimate the synchronization operator between D-PMU 1 at the substation and every other D-PMU i, where $i = 2;\dots;m+1$. Accordingly, we can express the optimization problem in (35) as follows:

$$k^? = \arg\min_p \sum_{i=2}^{m+1} \left| V_p^{f(1;i)} - V_p^{b(1;i)} \begin{bmatrix} V_1^{b(1;i)} & \dots & V_n^{b(1;i)} \end{bmatrix} \begin{bmatrix} V_1^{b(1;i)} \\ \vdots \\ V_n^{b(1;i)} \end{bmatrix} \begin{bmatrix} V_1^{f(1;i)} & \dots & V_n^{f(1;i)} \end{bmatrix} \begin{bmatrix} V_1^{f(1;i)} \\ \vdots \\ V_n^{f(1;i)} \end{bmatrix} \right|. \quad (36)$$

The methods in Section III.B for the case of H-PMUs and the methods in Section IV.B for the case of WMUs can be extended similarly to incorporate the use of several sensors.

It should be noted that, increasing the number of D-PMUs does not pose any considerable computational challenge. This is due to the fact that the proposed methods in this paper do not require using an optimization solver. Specifically, for the minimizations in (9), (12), (16), (26), and (29), we simply start from the bus where one sensor is located and go through the buses on the network topology until we reach the bus where the other sensor is located. Accordingly, we identify the location of the event by conducting a simple comparison of the objective function across the buses on such path. This would boil down to the light task of finding the smallest entry in a vector of up to n entries, where n is the total number of buses on the feeder. As for the minimization in (36), we do a similar light computation for the paths between the sensor at the substation and every other sensor. That is, we find the smallest entry in a matrix of up to $(m-1)\,n$ entries, where m is the total number of sensors. This is a light computation task and it does not require using an optimization solver tool.

B. Unbalanced Networks

The proposed methods can be readily applied to unbalanced three-phase networks. There are two options to consider. The first option is to apply the proposed methods to the positive sequence. This would be the most straightforward option.

The second option is to apply the proposed methods to each of the three phases, or to a sub-set of the three phases if the event is single-phase or double-phase. If we choose this second option to do the analysis separately on each phase, then we may observe redundancy in the results. For example, if the event is three-phase, then by applying the proposed methods to each of the three phases, we may obtain three separate results for the location of the event. In that case, we may use the average of such results, or we may consider the level of consistency among the results as a metric to assess confidence in the outcome of the event location identification task.

We will provide a comparison for the above two options in a case study on an unbalanced network in Section VI.G.

Fig. 5. The IEEE 33 bus test system with five sensors.

VI. Case Studies

In this section, we present several case studies to assess the performance of the proposed methods. Most case studies are applied to the IEEE 33 bus test system, with a main, three laterals, and five sensors, i.e., $m = 4$. Most case studies are done in PSCAD [34] to generate the sensor measurements. The event location identification methods are implemented in Matlab. The effectiveness of the event location identification methods is evaluated by using the following index:

$$\text{Inaccuracy Index} = \frac{1}{L}\sum_{l=1}^{L} \left| k_l^? - k_{l;\,\text{true}}^? \right|; \quad (37)$$

where L is the number of test cases, $k_l^?$ is the outcome of the event location identification method for test case l, and $k_{l;\,\text{true}}^?$ is the true location of the event for test case l. Clearly, the Inaccuracy Index considers not only whether the event location identification method is correct in each case, but also how far away the identified bus is from the true event bus.

A. Case Studies with D-PMUs

As mentioned in Section II, D-PMUs can identify the location of those events that cause a sustained change in the fundamental component of the voltage and/or current. In this section, we examine the ability of our proposed method to identify the location of two such events under the circumstances that we lose time synchronization among the D-PMUs.

1) Ground Fault: Suppose a single-line-to-ground fault occurs at bus 12. The fault resistance is 1. Suppose the D-PMUs have lost time synchronization before the fault occurs. Suppose the drift in time synchronization among the D-PMUs is 0.463 milliseconds; which is equivalent to $\theta = 10$ degrees. Fig. 6(a) shows the objective function in (35), as calculated at each bus, which is associated with the event location identification method in [4]. The minimum in this graph occurs at bus 10, which is not the correct event bus. Next, consider the graph in Fig. 6(b). It shows the objective function in (36),

Fig. 6. The results for estimating the event bus for a ground fault when D-PMUs have lost time synchronization, based on (a) the existing method in [4], and (b) the proposed method in Section II. The event occurs at bus 12.

TABLE I
DISTRIBUTION OF ERROR IN LOCATION IDENTIFICATION USING D-PMUS WHEN TIME SYNCHRONIZATION IS LOST

Method	Correct Bus	Neighboring Bus	Other Buses
[4]	66.72%	25.61%	7.67%
Proposed Method	89.29%	10.71%	0.00%

as calculated at each bus. This graph is obtained based on the proposed method in this paper. The minimum in this graph occurs at bus 12, which is the correct event bus. Therefore, our proposed method has identified the correct event bus despite lack of time synchronization among the D-PMUs.

Next, we repeat the above case study for different choices of the event bus and different choices of the amount of the drift in the time synchronization. In particular, we try 28 different cases for the location of the event bus, where can be any bus other than the buses that host the sensors. Also, we try 40 different cases for the drift in the phase angle difference due to lack of time synchronization, where can be any number between 30 degrees and 30 degrees, with 1.5 degrees increments. We assume that is the same between D-PMU 1 and D-PMUs 2, 3, 4, and 5. In total, we examine 28 40 = 1120 scenarios. The summary of the results are shown in Table I. As we can see, the method in [4] experiences major errors in identifying the event location, due to the impact of losing time synchronization among the D-PMUs. On the contrary, the proposed method almost always identifies the correct event location, while in some cases it identifies the immediate neighboring bus to the correct event bus.

Fig. 7(a) presents the Inaccuracy Index for the same case as a function of drift parameter which is caused by losing time synchronization among the D-PMUs. As we can see, increasing results in a significant increase in the Inaccuracy Index for the method in [4]. However, the proposed method in this paper remains robust against the changes in .

2) Capacitor Bank Switching: Turning on (i.e., energizing) and turning off (i.e., de-energizing) a capacitor bank can too cause a sustained change in the fundamental component of voltage and current. In this case study, we assume that the capacitor bank is 600 kVAR. We consider the same 1220 scenarios, as in the previous sub-section. Fig. 7(b) presents the

Fig. 7. Inaccuracy Index as a function of the drift in phase angle due to losing time synchronization for two different events that cause sustained changes on the fundamental phasors: (a) ground fault; (b) capacitor bank switching.

Inaccuracy Index as a function of drift parameter Again, we can see that increasing results in a major increase in the Inaccuracy Index for the method in [4], while the proposed method remains robust against the changes in .

B. Case Studies with H-PMUs

As mentioned in Section III, H-PMUs are effective in identifying the location of those events that cause a sustained change in the harmonic components of the voltage and current. In this section, we examine the ability of our proposed methods to identify the location of such events under the circumstances that we lose time synchronization among the H-PMUs.

1) High-Impedance Fault: Recall from Section III-B that we proposed two approaches to tackle losing time synchronization among H-PMUs. Approach 1 requires the presence of harmonics before the event occurs to allow estimating based on the harmonic measurements during the steady-state conditions before the event occurs. Accordingly, we use a current source at bus 18 to generate the third harmonics in the system. The magnitude is set to 1%, 2%, and 4% of the total magnitude of the current at the substation.

Table II shows the average Inaccuracy Index for 624 different scenarios, where the HIF can occur at 16 different locations, at buses 2 to 17, the DC voltage level inside the HIF model for the HIF can be 5 kV, 6 kV, and 7 kV, and the drift in the phase angle difference at the fundamental frequency can vary at 13 different levels between 0 to 60 degrees. Notice that, we cannot use Approach 1 in the absence of the background harmonics. That is why no result is included for Approach 1 under 0% background harmonics. However, Approach 2 is well-capable of assuring high-accuracy results in this case. Once we add the background harmonics to the system, Approach 1 too becomes applicable. In fact, in such cases, Approach 1 performs slightly better than Approach 2. For the results in Table II, we have also shown the Inaccuracy Index when D-PMUs are used. As we can see, the use of H-PMUs results in a much better performance than the use of D-PMUs, when it comes to identifying HIFs under the circumstances of losing time synchronization.

2) Utilizing Multiple Sensors: When it comes to H-PMUs, it is not common to have several sensors available on one feeder. Hence, for the results in Section VI.B.1, we assumed that only two H-PMUs are used. In this section, we expand the analysis to have five H-PMUs available on the network,

TABLE II
THE INACCURACY INDEX FOR IDENTIFYING THE LOCATION OF HIFS WHEN TIME SYNCHRONIZATION IS LOST

Sensor	Approach[y]	Background Harmonics (%)		
		0	2	4
		Inaccuracy Index		
H-PMUs	Approach 1	-	0.125	0.125
	Approach 2	0.167	0.167	0.188
D-PMUs[z]	-	0.229	0.229	0.229

[y] Approaches 1 and 2 are explained in Section III-B.
[z] Based on the proposed method in Section II.B.

Fig. 8. The results in identifying the location of HIFs by using H-PMUs when time synchronization is lost among the sensors (a) without using our proposed methods; and (b) with using our proposed methods.

at the locations marked on Fig. 5. The results are shown in Fig. 8. The HIF occurs at bus 12. Note that, the drift levels are presented in terms of $_1$ to have a single value on the x-axis, instead of based on $_3$ and $_5$. If our methods are not used, then the Inaccuracy Index increases as the drift in time synchronization increases. However, when our method is used, it works very efficiently and the Inaccuracy Index stays at zero.

C. Case Studies with WMUs

As mentioned in Section IV, WMUs can help in identifying the location of transient events that last for a short period of time, and cannot be identified by using D-PMUs and H-PMUs. In this section, we examine the ability of our method to find the location of such transient events under the circumstances that we lose time synchronization among the WMUs.

1) Incipient Fault: An incipient fault is a fault that is in its early stages. Many incipient faults manifest themselves in form of momentary (sub-cycle) arcing events [14, Section 4.3].

Suppose a sub-cycle incipient fault occurs at bus 9. Suppose it lasts for a quarter of a cycle, i.e., 4.16 milliseconds. Recall from Section IV that the key parameter to represent the drift in time synchronization for synchronized waveform measurements is . Assuming = 1:3 milliseconds, Fig. 9(a) shows the objective value in the minimization problem for event location identification based on the method in [15].

Fig. 9. The results for estimating the event bus for a sub-cycle incipient fault when WMUs have lost time synchronization, based on (a) the method in [15], and (b) the proposed method in Section IV. The event occurs at bus 9.

Fig. 10. Inaccuracy Index versus the drift in time synchronization of WMUs.

The minimum in this graph occurs at bus 7, which is not the correct event bus. Fig. 9(b) shows the objective value in the minimization problem for event location identification based on the proposed method. The minimum objective value for our method occurs at bus 9; which is the correct event bus.

Next, we plot the Inaccuracy Index when we vary from 2:5 milliseconds to +2:5 milliseconds. We also vary the event bus from bus 2 to bus 17. The results are shown in Fig. 10. We can see that the method in [15] is unable to accurately identify the correct location of the event when increases. On the contrary, the proposed method is capable of maintaining the high accuracy in event location identification despite the lack of time synchronization among the WMUs.

Notice that, the performance of the method in Fig. 10 is not symmetric with respect to negative and positive. The reason can be understood based on Fig. 4 in Section IV. When is negative, then the window to conduct modal analysis includes a displacement in the event signatures as seen by WMU 1 and WMU 2; yet it does not include any part of the waveforms before the event occurs. However, when is positive, then the window to conduct modal analysis does include part of the waveform before the event occurs. This causes a major error in the modal analysis, because the waveforms prior the occurrence of the event do not carry the oscillatory modes of the event. As a result, the Inaccuracy Index is significantly higher for the method in [15], when is positive.

2) Accuracy in Estimating : Next, we assess the ability of our method in estimating parameter . Fig. 11 shows the distribution of the error (in percentage) versus the true , where the true varies from 8:0 milliseconds to +8:0 milliseconds. The results here are averaged across the cases

Fig. 11. Distribution of the error in estimating the time drift parameter

Fig. 12. The results for estimating the event bus for an arcing fault that occurs at bus 10, when WMUs lose time synchronization, with = 2 milliseconds, based on (a) the method in [15], and (b) the proposed method in Section IV.

where the incipient fault occurs at various buses, from bus 2 to bus 17. We see that, either is very small, or the error in estimating is very small. That is why our method almost always obtains very high accuracy in identifying the event bus.

D. Arcing Fault

In this section, we do a case study based on an arcing fault. An arc fault is a nonlinear fault, e.g., see [35]. We simulated an arc fault in PSCAD using the existing PSCAD arc component [36]. Suppose the arc fault occurs at bus 10 in the IEEE 33 bus system. Both sensors are WMUs, where = 2 milliseconds. Note that, D-PMU and H-PMU may not be the right sensors in this case; because they may not identify the location of the arc fault even if time synchronization is not lost; given the sub-cycle nature of the arc fault. The results are shown in Fig. 12. We can see that the method in [15] identi es bus 12 as the event bus, which is incorrect. However, our proposed method identi es bus 10 as the event bus, which is correct.

E. The Relationship with Protection Devices

The proposed methods work not only for faults, which are the most severe events, but also various other events, such as incipient faults, high-impedance faults, or simple equipment or load switching. Regardless of the type of the event, the general assumption in this paper is that the measurements are obtained from multiple sensors. For the special case of analyzing faults, the measurements can also come from the existing protection devices and fault recorders that are available on the network. In fact, it is common for such devices to provide a few cycles before the fault trigger point as part of their fault capture mechanism. Further, most protection devices do not immediately trip during the rst fault cycle. For instance, they may wait until the third cycle from the start of the fault. This gives enough waveform capture in such devices under the fault conditions, which can be used for fault location identi cation using data from multiple protection devices.

Fig. 13. The results for estimating the event bus for an HIF at bus 14, when H-PMUs lose time synchronization, with = 20 , based on the method in Section III.B, and in the presence of a DER at bus 33 at the end of a lateral.

F. Systems with DERs

In this section, we examine the case where there is a sizeable DER on the power distribution feeder. Speci cally, we assume that a 250 kW PV unit is installed at bus 33 in the IEEE 33 bus test syste, i.e., at the end of a lateral. The rest of the settings in this case study is the same as those in Section VI.B. The event is assumed to be an HIF which occurs at bus 14. On average, we have = 20 for the four H-PMUs. The outcome of applying our proposed method from Section III.B in this scenario is shown in Fig. 13. As we can see, the proposed method nds the correct location of the event, despite the presence of the DER on the network in this scenario.

G. Larger and Unbalanced Three-Phase Networks

In this section, we conduct the analysis based on the IEEE 123 bus test system, which is unbalanced. The unbalance on this network is due to having unbalanced loads and unbalanced line parameters [37]. The network is shown in Fig. 14. There are four PMUs available on this network, as marked on the gure. For this case study, we examined three events, which are single-phase, double-phase, and three-phase. Therefore, not only the network is unbalanced, the events themselves are unbalanced too. The events are assumed to be capacitor bank switching, on one phase, on two phases, or on three phases, depending on the test case. A total of 100 test cases are considered for each type of event. These test cases are generated based on random choice of parameter between 30 and 30 . The results are summarized in Table III. Here, we compared the proposed method from Section II.B to the method in [4]. For the proposed method, we examine two options, namely to apply our method to the positive sequence, or to apply our method to the individual phases. These two options were previously explained in Section V.B. As we can see, these two options are equally good; and they both result in much better performance than using the method in [4].

H. Case Study based on Real-World Data

In this section, we evaluate our proposed method based on the real-world case study in [4, Section VI]. This case study includes identifying the location of a capacitor bank switching event on a power distribution feeder in California, based on measurements from two D-PMUs. The size of the capacitor

Fig. 14. The IEEE 123 bus test system, which is unbalanced, with 4 D-PMUs.

TABLE III
COMPARING DIFFERENT OPTIONS WHEN THE EVENTS ARE UNBALANCED

Method		Positive Sequence		Individual Phases	
Event Bus	Results	[4]	Sec. II.B	[4]	Sec. II.B
7	Correct	66	100	86	100
(Phases A and B)	Incorrect	34	0	14	0
27	Correct	52	100	66	100
(Phases A, B, C)	Incorrect	48	0	34	0
32	Correct	79	100	73	100
(Phase C)	Incorrect	21	0	27	0

bank is 900 kVAR. We use a simpli ed 8-bus network model of this real-world feeder, where the two D-PMUs are installed at bus 1 and bus 8. The capacitor bank switching takes place at bus 7. With $_1 = 10$, the results are obtained as shown in Fig. 15. As we can see, the method in [4] cannot identify the correct event bus due to lack of time-synchronization across the measurements. However, the proposed method, is able to identify the correct event bus, which is bus 7.

I. Computation Time

The proposed methods have light computational complexity. For example, the average computation time across 100 test cases for applying the proposed method on the IEEE 33 bus test system in Section II.B is 9.6 millisecond. As another example, for the larger network in Section VI.H, which is based on an unbalanced IEEE 123 bus test system, the average computation time across 100 test cases is 13.9 milliseconds. The above calculations are based on running the code for the proposed event location identi cation methods on Matlab version 2020a with an Intel Core i7-8700 CPU @ 3.20 GHz.

VII. CONCLUSIONS AND FUTURE WORK

We proposed ef cient methods to tackle losing time synchronization among advanced smart grid sensors, with focus on identifying the location of various events that may occur on power distribution systems. The proposed methods address

Fig. 15. A case study based on real-world D-PMU data, based on the experiment in [4, Section VI], but with $_1 = 10$ by using: (a) the method in [4]; and (b) the proposed method in Section III.B.

the unique challenges to this problem when it comes to each type of sensors, namely D-PMUs, H-PMUs, and WMUs. By properly de ning and estimating some synchronization factors in each case, we assured achieving comparable forward sweep and backward sweep calculations between a pair of sensors or among a group of sensors that lose time synchronization. Case studies based on the IEEE 33 bus test system showed that the existing methods suffer signi cant degradation in the accuracy of identifying the correct event bus, when D-PMUs, H-PMUs, or WMUs lose time synchronization. However, our proposed methods maintain high accuracy in all the cases.

The analysis in this paper can be extended in various directions. For example, while the focus here was on distribution feeders with a typical radial topology, one may consider networks with meshed or weakly meshed topologies. Of course, since the focus is on addressing lack of time synchronization among the sensors, one needs to rst identify an existing method that identi es the location of events in meshed or weakly meshed networks in the presence of time-synchronized measurements from multiple sensors. Such existing method can then be revised based on our proposed methods such that it can work well when time synchronization is lost.

As another example, the proposed methods in this paper could be extended to other applications in power system monitoring, i.e., beyond the task of event location identi cation. For instance, losing time synchronization can be a concern also in the state estimation problem, e.g., see [38], as well as the harmonic state estimation problem, e.g., see [39].

Finally, it will be insightful also to investigate how the issue of losing time synchronization can be addressed, when it is compared with (or combined with) the issue of bad data in power system monitoring. In general, bad data can happen due to failure in the sensor, in the data collection system, or in the communication infrastructure, among other factors. Bad data detection (and bad data correction) have been extensively studied in the literature, e.g., see the recent work in [40] for the case of bad data detection in D-PMUs. Accordingly, one may apply the existing bad data detection and the existing bad data correction methods to each individual sensor, prior to passing the data to the operator to conduct event location identi cation based on data from multiple sensors. Nevertheless, one may still have to examine the case where losing time

synchronization may happen when the system needs to also simultaneously deal with bad data at individual sensors.

REFERENCES

[1] K. Dehghanpour, Z. Wang, J. Wang, Y. Yuan, and F. Bu, "A survey on state estimation techniques and challenges in smart distribution systems," IEEE Trans. on Smart Grid, vol. 10, no. 2, pp. 2312–2322, 2019.

[2] A. von Meier, E. Stewart, A. McEachern, M. Andersen, and L. Mehrmanesh, "Precision micro-synchrophasors for distribution systems: A summary of applications," IEEE Trans. on Smart Grid, vol. 8, no. 6, pp. 2926–2936, 2017.

[3] H. Mohsenian-Rad, E. Stewart, and E. Cortez, "Distribution synchrophasors: Pairing big data with analytics to create actionable information," IEEE Power and Energy Magazine, vol. 16, no. 3, pp. 26–34, 2018.

[4] M. Farajollahi, A. Shahsavari, E. M. Stewart, and H. Mohsenian-Rad, "Locating the source of events in power distribution systems using micro-PMU data," IEEE Trans. on Power Systems, vol. 33, no. 6, pp. 6343–6354, 2018.

[5] Y. Zhang, J. Wang, and M. E. Khodayar, "Graph-based faulted line identi cation using micro-PMU data in distribution systems," IEEE Trans. on Smart Grid, vol. 11, no. 5, pp. 3982–3992, 2020.

[6] S. K.Jain, P. Jain, and S. N. Singh, "A fast harmonic phasor measurement method for smart grid applications," IEEE Trans. on Smart Grid, vol. 8, no. 1, pp. 493–502, 2017.

[7] A. Carta, N. Locci, and C. Muscas, "A pmu for the measurement of synchronized harmonic phasors in three-phase distribution networks," IEEE Transactions on Instrumentation and Measurement, vol. 58, no. 10, pp. 3723–3730, 2009.

[8] B. Zeng, Z. Teng, Y. Cai, S. Guo, and B. Qing, "Harmonic phasor analysis based on improved fft algorithm," IEEE Transactions on Smart Grid, vol. 2, no. 1, pp. 51–59, 2011.

[9] L. Chen, W. Zhao, F. Wang, and S. Huang, "Harmonic phasor estimator for p-class phasor measurement units," IEEE Trans. Instrum. Meas., vol. 69, no. 4, pp. 1556–1565, 2020.

[10] G. N. Lopes, V. A. Lacerda, J. C. M. Vieira, and D. V. Coury, "Analysis of signal processing techniques for high impedance fault detection in distribution systems," IEEE Trans. on Power Deliv., vol. 36, no. 6, pp. 3438–3447, 2021.

[11] M. Wei, F. Shi, H. Zhang, and W. Chen, "Wideband synchronous measurement based detection and location of high impedance fault in resonant distribution systems with integration of DERs," IEEE Trans. on Smart Grid, pp. 1–1, 2022.

[12] H. Mohsenian-Rad and W. Xu, "Synchro-waveforms: A window to the future of power systems data analytics," IEEE Power and Energy Magazine (accepted for publication), Apr. 2023.

[13] A. F. Bastos, S. Santoso, W. Freitas, and W. Xu, "Synchrowaveform measurement units and applications," 2019 IEEE Power Energy Society General Meeting (PESGM), 2019, pp. 1–5.

[14] H. Mohsenian-Rad, Smart Grid Sensors: Principles and Applications. Cambridge, UK: Cambridge University Press, April, 2022.

[15] M. Izadi and H. Mohsenian-Rad, "Synchronous waveform measurements to locate transient events and incipient faults in power distribution networks," IEEE Trans. on Smart Grid, vol. 12, pp. 4295–4307, 2021.

[16] M. Izadi and H. Mohsenian-Rad, "A synchronized lissajous-based method to detect and classify events in synchro-waveform measurements in power distribution networks," IEEE Trans. on Smart Grid, vol. 13, no. 3, pp. 2170–2184, 2022.

[17] M. Izadi and H. Mohsenian-Rad, "Characterizing synchronized Lissajous curves to scrutinize power distribution synchro-waveform measurements," IEEE Trans. Power Syst., pp. 1–4, May 2021.

[18] M. Izadi, M. J. Mousavi, J. M. Lim, and H. Mohsenian-Rad, "Data-driven event location identi cation without knowing network parameters using synchronized electric- eld and current waveform data," Proc. IEEE PES General Meeting, Denver, CO, 2022, pp. 1–5.

[19] W. Yao, Y. Liu, D. Zhou, Z. Pan, M. J. Till, J. Zhao, L. Zhu, L. Zhan, Q. Tang, and Y. Liu, "Impact of GPS signal loss and its mitigation in power system synchronized measurement devices," IEEE Trans. on Smart Grid, vol. 9, no. 2, pp. 1141–1149, 2018.

[20] W. Yao, D. Zhou, L. Zhan, Y. Liu, Y. Cui, S. You, and Y. Liu, "GPS signal loss in the wide area monitoring system: Prevalence, impact, and solution," Electric Power Systems Research, vol. 147, pp. 254–262, 2017.

[21] M. Gholami, A. Abbaspour, M. Moeini-Aghtaie, M. Fotuhi-Firuzabad, and M. Lehtonen, "Detecting the location of short-circuit faults in active distribution network using PMU-based state estimation," IEEE Trans. on Smart Grid, vol. 11, no. 2, pp. 1396–1406, 2020.

[22] X. Wang, H. Zhang, F. Shi, Q. Wu, V. Terzija, W. Xie, and C. Fang, "Location of single phase to ground faults in distribution networks based on synchronous transients energy analysis," IEEE Trans. on Smart Grid, vol. 11, no. 1, pp. 774–785, 2020.

[23] W. Qiu, H. Yin, L. Zhang, X. Luo, W. Wang, Y. Liu, W. Yao, L. Zhan, P. L. Fuhr, and T. J King, "Pulsar based timing for grid synchronization," IEEE Trans. on Ind. Appl., vol. 57, no. 3, pp. 2067–2076, 2021.

[24] Y. Wang and J. P. Hespanha, "Distributed estimation of power system oscillation modes under attacks on GPS clocks," IEEE Trans. Instrum. Meas., vol. 67, no. 7, pp. 1626–1637, 2018.

[25] A. S. Dobakhshari, "Wide-area fault location of transmission lines by hybrid synchronized/unsynchronized voltage measurements," IEEE Trans. on Smart Grid, vol. 9, no. 3, pp. 1869–1877, 2018.

[26] S. Lan, M.-J. Chen, and D.-Y. Chen, "A novel HVDC double-terminal non-synchronous fault location method based on convolutional neural network," IEEE Trans. on Power Deliv., vol. 34, pp. 848–857, 2019.

[27] P. Bountouris, H. Guo, D. Tzelepis, I. Abdulhadi, F. Coffele, and C. Booth, "MV faulted section location in distribution systems based on unsynchronized LV measurements," International Journal of Electrical Power Energy Systems, vol. 119, p. 105882, 2020.

[28] Z.-J. Ye, M. Farajollahi, and H. Mohsenian-Rad, "Impact analysis and mitigation of losing time synchronization at micro-PMUs in event location identi cation," in Proc. of the IEEE PES Innovative Smart Grid Technologies Conference, 2022, pp. 1–6.

[29] T.-C. Lin and Z.-J. Ye, "A signal-superimposed technique for fault location in transmission lines through IED measurements considering communication service failure," IEEE Systems Journal, vol. 15, no. 3, pp. 4525–4536, 2021.

[30] K. Kalita, S. Anand, and S. K. Parida, "A closed form solution for line parameter-less fault location with unsynchronized measurements," IEEE Trans. on Power Deliv., vol. 37, no. 3, pp. 1997–2006, 2022.

[31] C. A. Apostolopoulos, C. G. Arsoniadis, P. S. Georgilakis, and V. C. Nikolaidis, "Unsynchronized measurements based fault location algorithm for active distribution systems without requiring source impedances," IEEE Trans. on Power Deliv., vol. 37, no. 3, pp. 2071–2082, 2022.

[32] M. M. Saha, J. Izykowski, and E. Rosolowski, Fault location on power networks. London, U.K.: Springer, 2010.

[33] M. Farajollahi, A. Shahsavari, and H. Mohsenian-Rad, "Location identi cation of distribution network events using synchrophasor data," in 2017 North American Power Symposium (NAPS), 2017, pp. 1–6.

[34] "PSCAD." [Online]. Available: https://www.pscad.com/

[35] V. Terzija, G. Preston, V. Stanojevi, N. I. Elkalashy, and M. Popov, "Synchronized measurements-based algorithm for short transmission line fault analysis," IEEE Trans. on Smart Grid, vol. 6, no. 6, pp. 2639–2648, 2015.

[36] "PSCAD breaker arc model." [Online]. Available: https://www.pscad.com/knowledge-base/article/262

[37] "IEEE 123-Bus System." [Online]. Available: https://cmte.ieee.org/pes-testfeeders/resources/

[38] Y. Chen, J. Ma, P. Zhang, F. Liu, and S. Mei, "Robust state estimator based on maximum exponential absolute value," IEEE Trans. on Smart Grid, vol. 8, no. 4, pp. 1537–1544, 2017.

[39] I. D. Melo, J. L. R. Pereira, A. M. Variz, and P. A. N. Garcia, "Harmonic state estimation for distribution networks using phasor measurement units," Electric Power Systems Research, vol. 147, pp. 133–144, 2017 .

[40] A. Gholami, A. Vosughi, and A. K. Srivastava, "Denoising and detection of bad data in distribution phasor measurements using lters, clustering, and Koopman mode analysis," IEEE Trans. on Ind. Appl., vol. 58, pp. 1602–1610, Mar. 2022 .

Zong-Jhen Ye (S'20) received the M.S. degree in environmental engineering from National Cheng Kung University, Tainan, Taiwan, and second M.S. degree in electrical engineering from National Taipei University of Technology, Taipei, Taiwan. He is currently working toward the Ph.D. degree in electrical engineering at University of California, Riverside, CA, USA. His research interests are the applications of fault location techniques in transmission line and distribution systems.